Correlation between precipitation and the observation of giant aerosols over the Mediterranes basin

Pilar Gumà Claramunt and Fabio Madonna

1 Giant aerosol effects

Aerosol particles have diameters that span several orders of magnitude and they can be distinguished in different modes according to their diameters. They are usually divided into four modes: the nucleation mode, the Aitken mode, the accumulation mode, and the coarse mode, as shown in Fig. 1. Anthropogenic aerosols occur mainly in submicron range, and natural aerosols in the supermicron range: soot and sulphuric acid are Aitken particles, while biomass burning smoke usually falls into the accumulation mode; mineral dust, sea salt, pollen and volcanic particles are coarse.

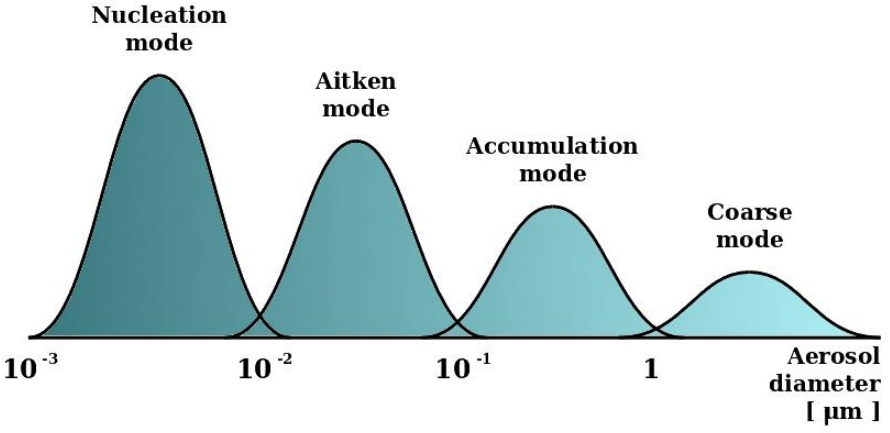

Figure 1: Aerosol modes

Atmospheric aerosol particles serve as condensation nuclei for the formation of both, cloud droplets and atmospheric ice particles. As a result, they exert a substantial influence on the microphysical properties of water and ice clouds, which in turn affect the processes that lead to the formation of rain, snow, hail, and other forms of precipitation.

Increased Cloud Condensation Nuclei (CCN) load due to anthropogenic activity might lead to non-precipitating clouds (e.g. aerosol indirect effect) because the cloud drops become smaller (for a constant liquid water content) and, therefore, less efficient in rain formation (aerosol indirect effect). Adding giant CCN (GCCN), larger than 5 microns, into such a cloud can initiate precipitation (namely, drizzle) and, therefore, might counteract the aerosol indirect effect.

The impact of GCCN on the formation of precipitation is the subject of various studies. Giant and ultra-giant CCN may produce a tail of large droplets within the cloud droplet distribution. The resulting cloud droplets take part in collision/coalescence processes.

Very large drops (~60−100 µm) contribute most to the precipitation formation because they have a high level of collection.

Giant aerosols (e.g. diameter larger than 5 microns) can also act as IN, affecting the temperature at which ice nucleation occurs.

Hence, to fulfil the objective of the OSCAR projects, precipitation measurements performed at a regional scale have been correlated with the observation of GCCN [2]. This approach implies that each aerosol outbreak occurring over Basilciata region is assumed to distributed at the mesoscale over a regional area.

2. Rain gauges

The accumulated precipitation in the Basilicata region where the study has been carried out was measured by the rain gauges network (Fig. 2) run by by Italian Depertment of Civil Protection.

The rain gauges network run by the Basilicata Region Civil Protection measures the accumulated precipitation in the region where the study has been carried out with an accuracy of 0.2 mm. Figure 2 shows all the rain gauges that have been considered.

There are several hydrological basins in the Basilicata region, and for this reason the pluviometers have been divided in three groups according to the regions used by Civil Protection to emit hydrogeological risk regional warnings [8]:

• Group A

comprises the hydrological basins in the north and northwest of the region, corresponding to the rivers Ofanto and Sele;

• Group B

contains the eastern area of the region, in the Basento,Bradano and Cavone rivers domain;

• Group C

embraces the southern part of the region, including the Agri, Noce and Sinni hydrological basins.

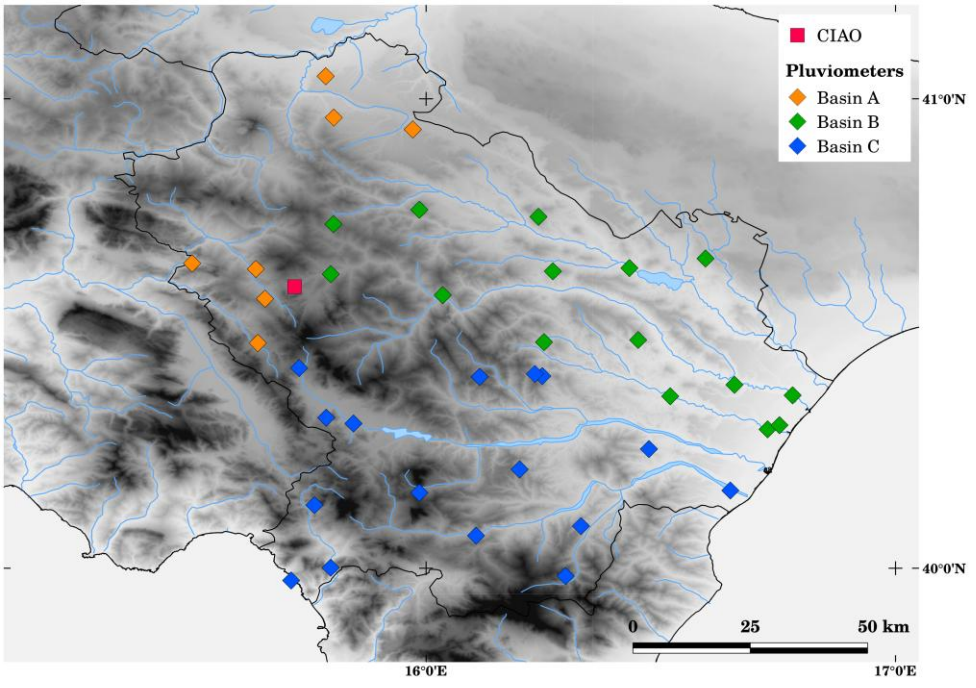

Figure 2: Rain gauges network of the Basilicata region, run by the Civil Protection in the Basilicata region. The rain gauges are divided into the three hydrological basins, indicated with A, B and C.

3. Precipitation

A dataset of cases characterized by the idenfitication of aerosol giant particles [4] has been used to correlate the accumulated rain at the regional scale with the observation of giant aerosol by the CNR-IMAA Atmospheric Observatory (CIAO), run by CNR in Tito Scalo, Potenza [5]. In Fig. 3, the frequency distribution of accumulated rain in the three hydrological basins, described in Fig. 2, during the 24 hours following the event (giant or not giant) is shown. Note that the percentage of cases with precipitation is approximately 15% lower after giant aerosol events. Accordingly, the accumulated rain after giant aerosols is also lower. On the other hand, higher values of precipitation rain rate are observed after the presence of giant aerosols (Fig. 4).

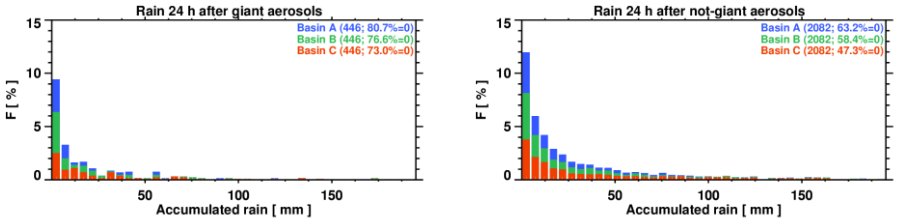

Figure 3: Total accumulated rain in the three hydrological basins in presence of (a) giant and (b) not giant aerosol in the 24 hours following the events. In parenthesis, the number of cases considered in the statistics for each basin together with the percentage of events without precipitation are noted.

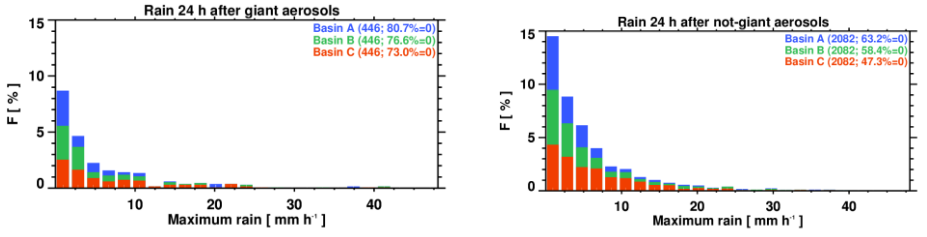

Figure 4: Maximum rain rate in the three hydrological basins in presence of (a) giant and (b) not giant aerosol in the 24 hours following the events. In parenthesis, the number of cases considered in the statistics for each basin together with the percentage of events without precipitation are noted.

The relation between the total amount of precipitation and the maximum rain rate is presented in Figure 5. It is shown that, even if the amount of accumulated precipitation is lower after aerosols observations, the rate between the maximum and the accumulated rain is higher. This means that the probability of rain showers is higher after the observation of giant aerosols. This finding might be linked to the aerosol indirect effect as an evidence of the fact the giant aerosol speed up the droplet activation process and the related warm rain process with a consequent shorter cloud lifetime.

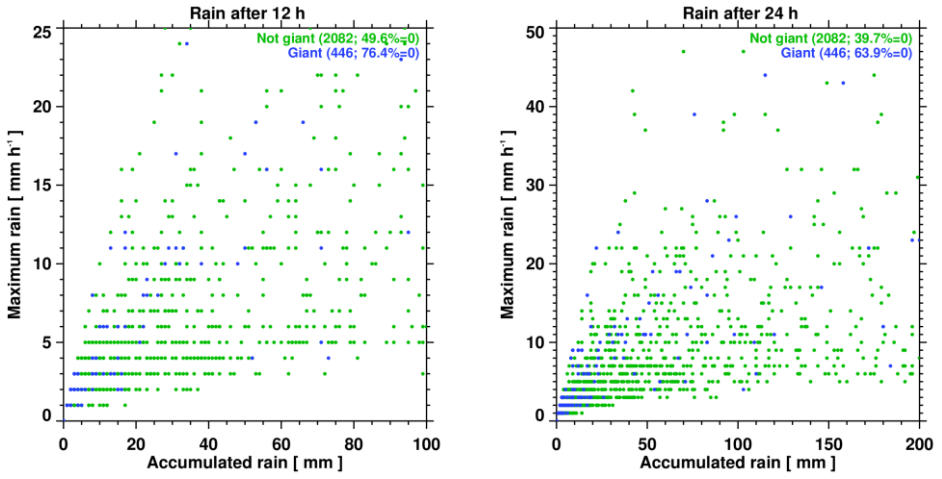

Figure 5: Total accumulated rain in all the basins versus maximum rain rate for giant and not giant observations in the following (a) 12 and (b) 24 hours. In absence of giant particles, the time interval starts after a random hour of the day. In parenthesis, the number of cases considered in the statistics with the percentage of events without precipitation are reported.

In Figure 6, the temporal evolution of the accumulated rain and the maximum rain rate occurrence are reported. The accumulated precipitation (Fig. 6a) is lower after giant aerosol observations, while there are not major differences in the time evolution. In the occurrence in time of the maximum rain rate (Fig. 6b), though, this changes: the maximum rain rate is preferentially observed from 30 to 40 hours after giant observations, while it seems there is not any evident maximum value of the rain rate in absence of giant particles. The same effect is observed for all the hydrological basins (Fig. 7).

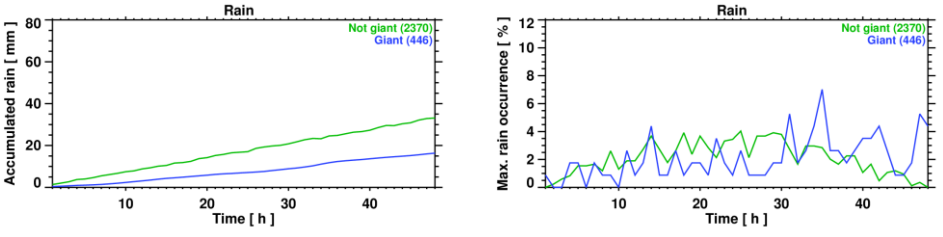

Figure 6: Evolution of (a) total accumulated rain and (b) maximum rain rate occurrence in time during the 48 hours after giant and not-giant events. In parenthesis, the number of cases for each type.

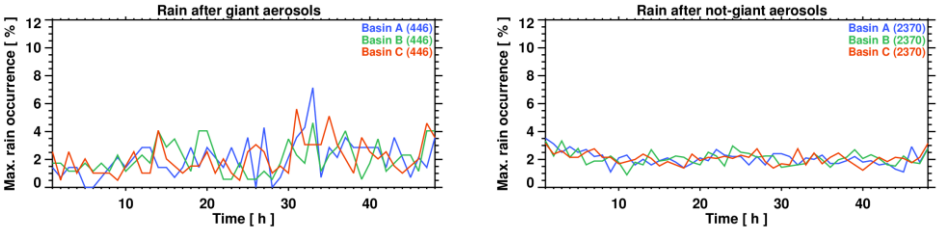

Figure 7: Evolution of maximum rain rate occurrence in time during the 48 hours after (a) giant and (b) not giant events for each hydrological basin. In parenthesis, the number of cases considered.

4. Fog events

A statistics on the occurrence fog at CIAO observatory is presented in this section in order to investigate the impact of diurnal fog on the solar irradiance. The frequency and the intensity of this event may condition the exploitation of solar energy

In Fig. 8, it is reported the probability density functions of the altitude of the cloud ceiling measured by the VAISALA CT25K laser ceilometer operational at CIAO during the year 2014. Ceilometer technology is well described in [6, 7]. The lower panel includes only the daytime data. The pdf corresponding to the first bin include all the cases with a cloud base lower than 100 m and, therefore, classified as fog events.
Cloudiness covers 42 % of the year during night and day, while during the this value increases up to 46 %.
The pdfs show a value of 0.22 for the observation of fogs during night and day over one year corresponding to about 60 hours of fog. During daytime, we have a value of 0.12 corresponding to about 18 hours of fog.
So we may conclude that at least for the CIAO site the fog is not frequently occurring . this in any case demonstrates how lidar elastic lidar sensors may detect the fog easily and OSCAR prototype can be used for this purpose.

Finally it is worth to precise that fog effect on the solar irradiance also depends on the thickness of the fog. OSCAR lidar can also estimate the value of the fog optical depth using both lidar scanning measurements and the algorithm based on the pyranometer measurements [1, 3], included in the OSCAR prototype.

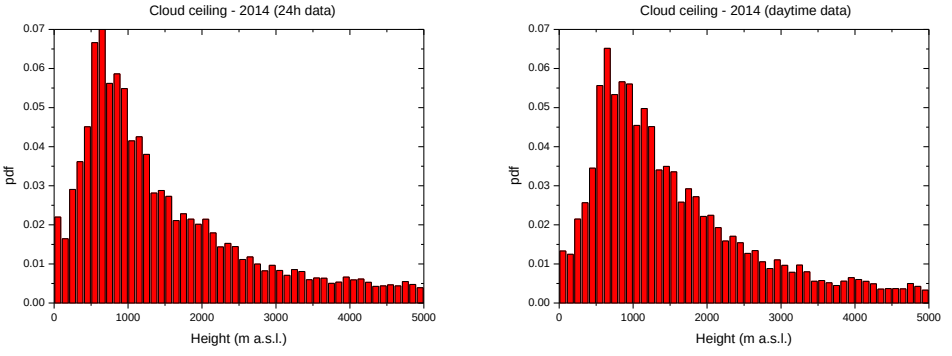

Figure 8: probability density functions of the cloud ceiling measured by the VAISALA CT25K laser ceilometer operational at CIAO during the year 2014. The right panel includes only the daytime data. The pdf corresponding to the first bin include all the cases with a cloud base lower than 100 m and classified as fog events.

5. Conclusions

The effects of aerosols and in particular of GCCN on the regional meteorology have been studied. The following conclusion can be drawn from the presented data analysis regarding the relationship between aerosol and precipitation:

a. the presence of giant aerosol decrease the percentage of cases with precipitation and, accordingly, the accumulated rain of approximately 15% with respect to finer particles;

b. higher values of precipitation rain rate are observed in presence of giant aerosol, i.e. the probability of rain showers is higher;

c. the maximum rain rate is preferentially observed from 30 to 40 hours after the observation of giant aerosol, while it seems there is not any evident maximum value of the rain rate in absence of giant particles.

And regarding the effect of fog on the solar irradiance:

d. at CIAO site the fog is not frequently occurring, and therefore does not represent a critical issue for the exploitation of the solar energy.

The presented studied will be extended over the whole historical data archive of measurements available the CIAO and then published in peer-reviewed literature.

6. References

[1] Chiu, J. C., A. Marshak, Y. Knyazikhin, W. Wiscombe, H. Barker, J. C. Barnard, and Y. Luo (2006), Remote sensing of cloud properties using ground-based measurements of zenith radiance, J. Geophys. Res., 111, D16201, doi:10.1029/2005JD006843.

[2] Gumà-Claramunt, P. (2015). Synergy between Doppler radar and Raman lidar for aerosol investigation. PhD thesis, Methods and technologies for environmental monitoring, University of Basilicata.

[3] Li, Z., F. Zhao, J. Liu, M. Jiang, C. Zhao,and M. Cribb (2014), Opposite effects of absorbing aerosols on the retrievals of cloud optical depth from spaceborne and ground-based measurements, J. Geophys. Res. Atmos., 119, doi:10.1002/ 2013JD021053.

[4] Madonna, F., A. Amodeo, G. D'Amico, and G. Pappalardo (2013), A study on the use of radar and lidar for characterizing ultragiant aerosol, Journal of Geophys. Res., DOI: 10.1002/jgrd.50789.

[5] Madonna, F., Amodeo, A., Boselli, A., Cornacchia, C., Cuomo, V., D'Amico, G., Giunta, A., Mona, L., and Pappalardo, G.: CIAO: the CNR-IMAA advanced observatory for atmospheric research, Atmos. Meas. Tech., 4, 1191-1208, doi:10.5194/amt-4-1191-2011, 2011.

[6] Madonna, F., Amato, F., Vande Hey, J., and Pappalardo, G.: Ceilometer aerosol profiling versus Raman lidar in the frame of the INTERACT campaign of ACTRIS, Atmos. Meas. Tech., 8, 2207-2223, doi:10.5194/amt-8-2207-2015, 2015.

[7] Wiegner, M., Madonna, F., Binietoglou, I., Forkel, R., Gasteiger, J., Geiß, A., Pappalardo, G., Schäfer, K., and Thomas, W.: What is the benefit of ceilometers for aerosol remote sensing? An answer from EARLINET, Atmos. Meas. Tech., 7, 1979–1997, doi:10.5194/amt-7-1979-2014, 2014.

[8] http://www.protezionecivilebasilicata.it/protcivbas/home.jsp.